ACS chemical biology

Articles

pubs.acs.org/acschemicalbiology

Pyrimidyn Compounds: Dual-Action Small Molecule Pyrimidine-Based Dynamin Inhibitors

Andrew B. McGeachie,[†,○,#] Luke R. Odell,[‡,○,#] Annie Quan,[†] James A. Daniel,[†] Ngoc Chau,[†] Timothy A. Hill,[‡,○] Nick N. Gorgani,[†] Damien J. Keating,[∥] Michael A. Cousin,[∥] Ellen M. van Dam,[§] Anna Mariana,[‡] Ainslie Whiting, Swetha Perera,[†] Aimee Novelle,[†] Kelly A. Young,[‡] Fiona M. Deane,[‡] Jayne Gilbert,[¶] Jennette A. Sakoff,[¶] Megan Chircop,[†] Adam McCluskey,[‡] and Phillip J. Robinson*[,†]

[†]Cell Signalling Unit, Children's Medical Research Institute, The University of Sydney, Sydney, NSW 2145, Australia

[‡]Centre for Chemical Biology, Chemistry, The University of Newcastle, Callaghan, NSW 2308, Australia

[§]The Garvan Institute, 384 Victoria Street, Darlinghurst, Sydney, NSW 2010, Australia

[∥]Department of Human Physiology, Flinders University, Adelaide, South Australia, 5001, Australia

[⊥]Centre for Integrative Physiology, George Square, University of Edinburgh, Edinburgh EH8 9XD, U.K.

[¶]Department of Medical Oncology, Calvary Mater Newcastle Hospital, Waratah, NSW 2298, Australia

Supporting Information

ABSTRACT: Dynamin is required for clathrin-mediated endocytosis (CME). Its GTPase activity is stimulated by phospholipid binding to its PH domain, which induces helical oligomerization. We have designed a series of novel pyrimidine-based "Pyrimidyn" compounds that inhibit the lipid-stimulated GTPase activity of full length dynamin I and II with similar potency. The most potent analogue, Pyrimidyn **7**, has an IC_{50} of 1.1 μM for dynamin I and 1.8 μM for dynamin II, making it among the most potent dynamin inhibitors identified to date. We investigated the mechanism of action of the Pyrimidyn compounds in detail by examining the kinetics of Pyrimidyn **7** inhibition of dynamin. The compound competitively inhibits both GTP and phospholipid interactions with dynamin I. While both mechanisms of action have been previously observed separately, this is the first inhibitor series to incorporate both and thereby to target two distinct domains of dynamin. Pyrimidyn **6** and **7** reversibly inhibit CME of both transferrin and EGF in a number of non-neuronal cell lines as well as inhibiting synaptic vesicle endocytosis (SVE) in nerve terminals. Therefore, Pyrimidyn compounds block endocytosis by directly competing with GTP and lipid binding to dynamin, limiting both the recruitment of dynamin to membranes and its activation. This dual mode of action provides an important new tool for molecular dissection of dynamin's role in endocytosis.

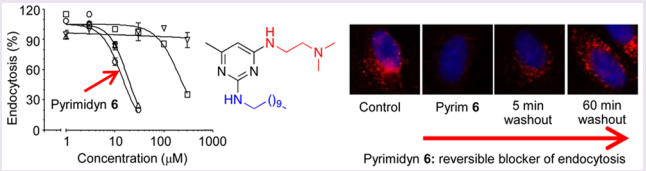

Endocytosis is a process in which the plasma membrane is selectively deformed inward to form intracellular lipid-bound vesicular structures.[1] It acts as both a retrieval mechanism for the recycling of membrane and embedded components as well as a means for the capture of extracellular material in the form of internalized cargo.[2,3] These vesicles come in a variety of forms, ranging from large phagosomes to small clathrin-coated vesicles, including the smallest, synaptic vesicles. There are a variety of mechanisms for endocytosis, with the best characterized being clathrin-mediated endocytosis (CME) of activated, ligand-bound membrane receptors.[1] CME requires a clathrin cage to shape the vesicle size and the large GTPase dynamin II for vesicle neck fission.[4] A molecular variant of CME is synaptic vesicle endocytosis (SVE), which is confined to presynaptic nerve terminals and is regulated by dynamin I and utilizes a similar CME machinery but mainly with neuron-specific variants of many of the proteins.[5,6]

Dynamin consists of five functional domains: (i) the G domain, which binds and hydrolyses GTP resulting in the mechanical release of the vesicle; (ii) the Bundle Signaling Element (BSE)/GTPase effector domain (GED) which appears to be responsible for the self-assembly of dynamin[7] and acts as a GTPase activator protein to stimulate GTPase activity;[8] (iii) the stalk (also known as the middle domain); (iv) the pleckstrin homology (PH) domain, which targets dynamin to the membrane by interacting with lipids and may also act as a GTPase inhibitory module;[9] and (v) the proline-rich domain (PRD), which is involved in the binding of dynamin to a number of SH3 containing proteins as well as the site of *in vivo* phosphorylation.[10,11] In CME, dynamin is recruited to the invaginating vesicle, where assembly into a helical structure occurs around the vesicle neck.[12] Dynamin requires its PH domain to target sites of endocytosis[5,13,14] that have a hydrophobic loop that inserts into the lipid bilayer for

Received: February 25, 2013
Accepted: May 3, 2013
Published: May 3, 2013

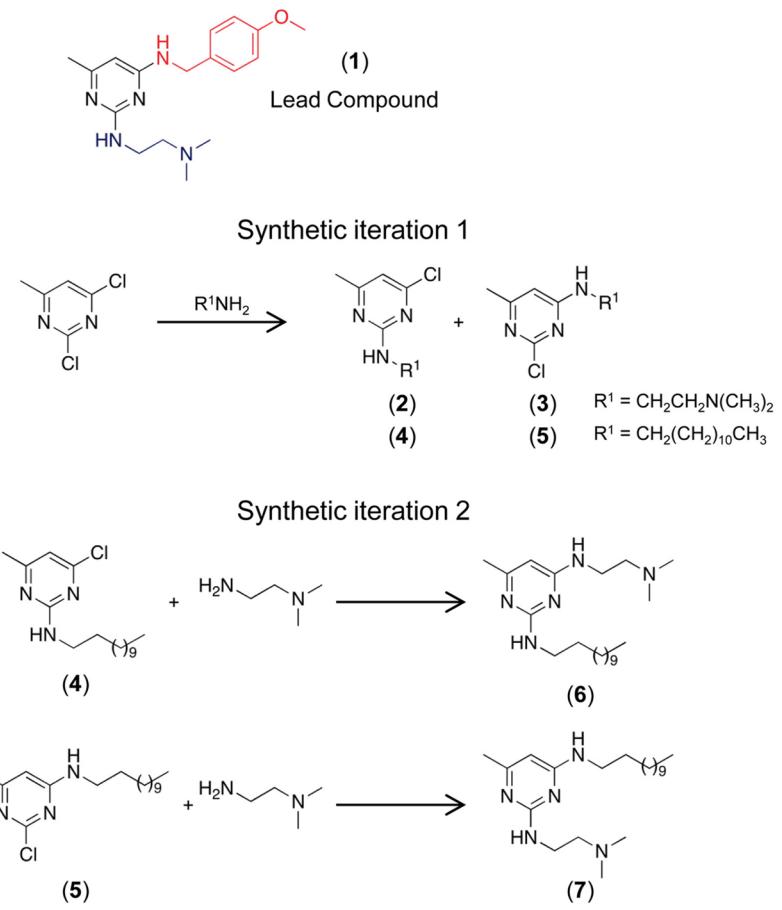

Figure 1. Lead compound **1** and subsequent library design, synthesis, and development of **6** and **7** as potent dynamin I GTPase inhibitors.

membrane curvature generation.[15] GTP hydrolysis triggers a conformational constriction, and the vesicle is cut from the plasma membrane.[16−18]

Many classical inhibitors of endocytosis lack a well-defined mechanism of action.[19] Nonspecific inhibitors include cationic amphiphilic drugs (e.g., chlorpromazine),[20] concanavalin A, phenylarsine oxide,[21] dansylcadaverine,[22] intracellular potassium depletion,[23] intracellular acidification,[24] and decreasing medium temperature to 4 °C.[25] Their low potency and lack of a specific target have led to the development of small molecules with defined target proteins, in particular, clathrin[26] and dynamin.[27] We have developed a number of classes of dynamin inhibitors, including long chain ammonium salts (MiTMAB analogues),[28] room-temperature ionic liquids (RTILs),[29] Dynole analogues,[30,31] Iminodyn analogues,[32] Pthaladyn analogues,[33] Rhodadyn analogues,[34] and the Dyngos,[35] which are more potent analogues of dynasore.[36] Each inhibitor series is chemically distinct, with different targets within dynamin.[27] The inhibitors described to date affect the PH domain and interfere with interaction of dynamin with phospholipids (MiTMAB compounds and RTILs),[28,37] the G domain by competing with GTP (Pthaladyn analogues), or allosterically inhibit the GTPase activity (Dynole, Dyngo, Iminodyn and Rhodadyn analogues).

We now report a new series of novel dynamin inhibitors called the Pyrimidyn series. They are substituted pyrimidine compounds that also incorporate some design aspects of pre-existing dynamin inhibitors that target either the PH domain or the GTPase domain. As the Pyrimidyn analogues are nucleotide analogues,[38−40] they competitively target the GTP binding pocket; however, they also share structural similarities with the ammonium salt inhibitors,[28] conferring amphiphilic properties that interfere with dynamin binding to phospholipids. Thus, the Pyrimidyn analogues are the first dual-action dynamin inhibitors.

RESULTS AND DISCUSSION

Development of the Pyrimidyn Analogues: Pyrimidine-Based Inhibitors of Dynamin. Prior development of libraries of corticotrophin-releasing hormone antagonists within our laboratories[52] resulted in the development of a wide range of substituted pyrimidines.[53,54] Given that pyrimidines are known to function as nucleotide mimetics,[38−40] we reasoned that these compounds may have utility in the development of inhibitors against the GTP binding site of dynamin. We therefore screened our existing pyrimidine libraries for inhibition of dynamin I and identified Pyrimidyn **1** as a 35.3 ± 7.1 μM dynamin I inhibitor (Supplementary Table S1). Although a relatively poor inhibitor compared to those we had previously developed,[28,37,55,56] we were sufficiently encouraged to further develop a targeted library that we refer to as the Pyrimidyn series. Commencing with commercially available 2-methyl-4,6-dihydroxypyrimidine, we generated the required 4,6-dichloro analogue. Treatment of this material as previously reported[54] at RT with 1 equiv of amine gave rise to an easily separable mixture of monosubstituted 2- and 4-amino pyrimidines (Figure 1). Evaluation of this first iteration highlighted three analogues, Pyrimidyn **2**, **3** and **5**, with 1.2-

dx.doi.org/10.1021/cb400137p | ACS Chem. Biol. 2013, 8, 1507−1518

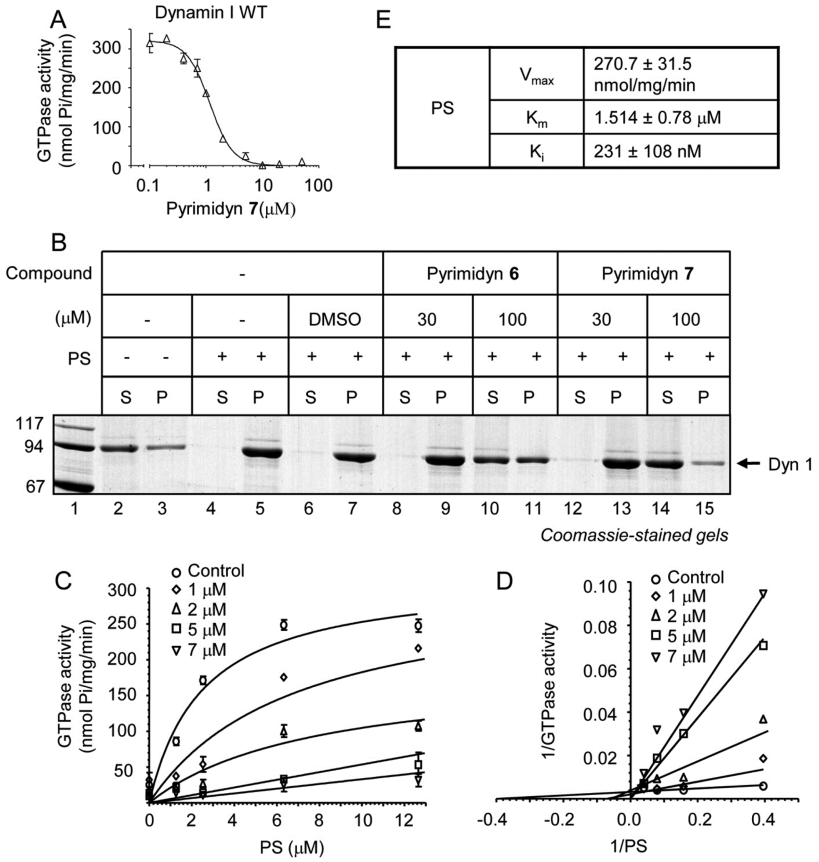

Figure 2. Pyrimidyn **6** and **7** inhibit the GTPase activity of dynamin I by disrupting PH domain interactions with lipids. (A) The PS-stimulated GTPase activity of native sheep brain dynamin I (WT, 20 nM) was determined in the presence of a range of concentrations of Pyrimidyn **7**. An IC_{50} value of 1.1 μM was obtained from the resulting IC_{50} curve. (B) *In vitro* phospholipid binding of WT dynamin in the presence of Pyrimidyn **6** or **7**. Normal binding of dynamin to phospholipids is indicated by its presence in the pellet (P) fraction compared to the supernatant (S) fraction. The Coomassie-stained polyacrylamide gel shown is representative of 3 independent experiments. (C) Michaelis–Menten and (D) Lineweaver–Burke plots showing the effect of Pyrimidyn **7** on dynamin I GTPase with increasing concentrations of PS liposomes and GTP concentration (300 μM). This data shows that the compound is a PS-competitive inhibitor of dynamin I. (E) Michaelis–Menten constants V_{max}, K_m, and K_i (±95% CI) were calculated from triplicate samples performed during a single experiment. Error bars in all graphs represent SEM (n = 3 independent experiments).

to 6-fold increases in dynamin I inhibition relative to the lead compound (Supplementary Table S1). Introduction of the dimethylaminoethyl side chain led to the production of two regioisomers with increased potency in comparison to that of lead Pyrimidyn **1**, with Pyrimidyn **3** three times as potent as Pyrimidyn **2**. Introduction of a dodecyl side chain as in Pyrimidyn **4** had no effect on dynamin inhibition (this was also observed with the corresponding C4 isomer; data not shown). This suggested that introduction of a second amino substituent may further improve potency. We viewed the synthesis of a Pyrimidyn **2**/**3** and **5** hybrid as a logical strategy in developing more potent inhibitors. Accordingly, Pyrimidyn **6** and Pyrimidyn **7** were synthesized from Pyrimidyn **4** and Pyrimidyn **5**, respectively, via treatment with *N*,*N*-dimethylethylenediamine. Evaluation of Pyrimidyn **6** and **7** realized a further 4- to 16-fold increase in dynamin inhibition. The full dose–response curve for Pyrimidyn **7** is shown in Figure 2A.

We further examined whether these compounds exhibited equipotent inhibition of both dynamin I and II. IC_{50} values cannot readily be compared for two different enzymes unless they and their relevant cofactors and activators are present at the same concentrations. To do this, the GTPase assays for dynamin I and II were normalized (modified such that they yielded similar quantities of phosphate released using identical amounts of dynamin protein). This allows direct comparison of the IC_{50} values from the two assays. After assay normalization, no selectivity was observed for **6** or **7**, with both inhibitors potently inhibiting dynamin I and II with nearly the same potencies (Supplementary Table S2).

The Pyrimidyn Series Competitively Inhibit Binding of Both GTP and Phospholipid. We next examined the mechanism of Pyrimidyn **7** inhibition of dynamin I. Phosphatidylserine (PS) binds to the PH domain of dynamin and enhances its GTPase activity[57,58] by inducing cooperative helix oligomerization.[59] The MiTMAB series of compounds are surface-active, expected to interfere with protein–lipid interactions,[60,61] and have been shown to compete for PS binding to the dynamin I PH domain.[37] Structural similarities between the MiTMAB and Pyrimidyn series, such as the presence of an extended carbon chain, led us to investigate whether the latter also target the dynamin–phospholipid interaction. In a sedimentation assay, we found that when dynamin was mixed with liposomes and centrifuged, dynamin was located almost entirely in the pelleted lipid fraction (Figure 2B, lanes 4 and 5). Addition of 30 μM concentration of either **6** or **7** did not change this distribution; however, at 100 μM both compounds caused the majority of dynamin to remaining in the supernatant fraction (Figure 2B). This suggests that both

dx.doi.org/10.1021/cb400137p | *ACS Chem. Biol.* 2013, 8, 1507–1518

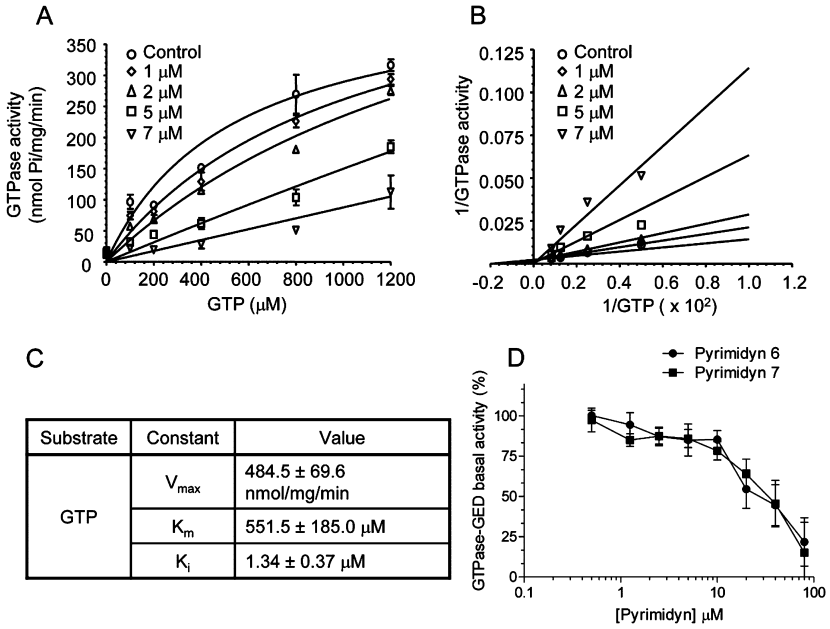

Substrate	Constant	Value
GTP	V_{max}	484.5 ± 69.6 nmol/mg/min
	K_m	551.5 ± 185.0 μM
	K_i	1.34 ± 0.37 μM

Figure 3. Pyrimidyn **7** is a competitive dynamin I inhibitor with both GTP and PS. (A) Michaelis–Menten and (B) Lineweaver–Burke plots showing the effect of varying concentrations of **7** on the GTPase activity of WT dynamin I (20 nM), under conditions of increasing GTP concentration and a fixed PS concentration (12.7 μM). This data shows that Pyrimidyn **7** acts as a GTP-competitive inhibitor of dynamin I. (C) Michaelis–Menten constants V_{max}, K_m, and K_i (±95% CI) were calculated from triplicate samples performed during a single experiment. Pyrimidyns inhibit basal GTPase activity. (D) Effects of different amounts of Pyrimidyn **6** (●) and Pyrimidyn **7** (■) on GTPase activity of GTPase-GED (2000 nM) for 60 min is depicted. All results are representative of at least 2 independent experiments. Error bars represent SEM.

Pyrimidyn **6** and **7** interfere with the interaction of dynamin with lipids. To investigate whether Pyrimidyn analogues were able to compete with PS for dynamin I binding, thereby inhibiting GTPase activity, we tested the effect of systematically varying the concentration of both Pyrimidyn **7** and PS on the kinetics of dynamin I GTPase activity, while using a fixed concentration of GTP. Addition of increasing concentrations of **7** did not change the V_{max} and increased the K_m, showing, in combination with Lineweaver–Burke double reciprocal plots, that **7** competitively inhibited the activation of dynamin I by PS (Figure 2C–E).

Given that the compounds are pyrimidine analogues, it was also possible that the Pyrimidyns could inhibit dynamin I by competing with GTP binding. Therefore, the kinetics of dynamin I GTPase activity was investigated while varying both the concentration of Pyrimidyn **7** and GTP, while maintaining a constant PS concentration. Pyrimidyn **7** acted in competition with GTP for binding to dynamin (Figure 3A–C). Taken together, these data demonstrated that the Pyrimidyn compounds possess a dual mechanism of activity, inhibiting dynamin interaction with lipid and also competing for GTP binding.

We investigated whether the Pyrimidyns were capable of inhibiting basal dynamin activity or whether they were only effective on stimulated dynamin activity. To do this, we performed GTPase assays using the dynamin GTPase-GED construct, which both lacks a PH domain and is incapable of assembling into multimeric structures, therefore exhibiting only basal GTPase activity.[44] We found that Pyrimidyns **6** (IC_{50} = 50 μM) and **7** (IC_{50} = 85 μM) both inhibited GTPase activity of the GTPase-GED construct (Figure 3D). The IC_{50} values for both Pyrimidyns using 2000 nM GTPase-GED were ~40-fold higher than experiments using 20 nM full-length dynamin (Supplementary Table S1), consistent with the high concentration of the GTPase-GED construct we needed to use in these assays to remain within the assay's dynamic range. Therefore the Pyrimidyns inhibit both basal and PS-stimulated activity with approximately the same potency, consistent with the compounds' GTP-competitive mechanism of action.

Pyrimidyn Compounds Block CME in Non-neuronal Cells. Treatment of cells with dynamin inhibitors leads to a decrease in CME.[27] The effect of Pyrimidyn compounds on CME was examined by monitoring the uptake of transferrin (Tf) and epidermal growth factor (EGF) in COS7 cells. Both Pyrimidyn **6** and **7** (30 μM) produced a dramatic reduction in EGF-A488 and Tf-TXR internalization (Figure 4A). Pyrimidyn **5** (30 μM), a relatively weak inhibitor of dynamin GTPase activity, had no effect on CME. The same results were observed for EGF-A488 uptake in HER14 cells.

The effects were then quantified at different drug concentrations using a semiautomated CME assay. The IC_{50} for inhibition of CME by Pyrimidyn **7** in COS-7 cells was 12.1 ± 2.1 μM and Pyrimidyn **6** was slightly less potent (19.6 ± 3.5 μM) (Figure 4B). The assay was also carried out using U2OS cells and generated similar IC_{50} values (Supplementary Table S1). For comparison, the parent Pyrimidyn **1** was ~20 times less potent than **7** (211 ± 37.1 μM), and **5** had no effect on CME. The observations are in accordance with the relative potency of Pyrimidyn compounds on dynamin GTPase activity, suggesting they block CME by inhibition of dynamin. The Pyrimidyn compounds do not influence total cellular EGF receptor expression levels or EGF receptor activation in A431 cells (Supplementary Figure S1), precluding the possibility that these observations were due to an effect on EGF receptor signaling. The inhibitory effects of Pyrimidyn **6** and **7** on CME were reversible, with 40% recovery after 5 min and 80% recovery after 60 min of removal of the compound (Figure 4C

dx.doi.org/10.1021/cb400137p | ACS Chem. Biol. 2013, 8, 1507–1518

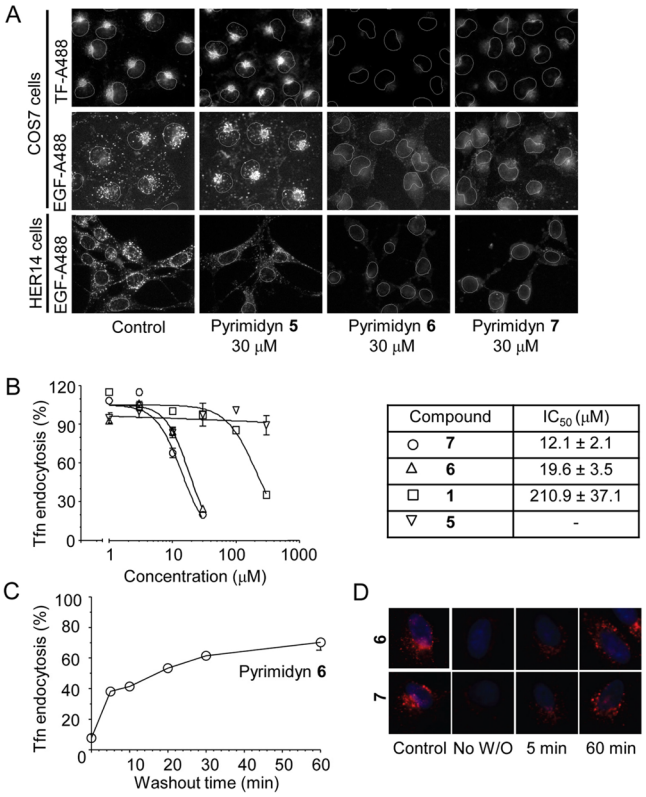

Figure 4. Pyrimidyn **6** and **7** reversibly inhibit CME in cultured cells. (A) CME was analyzed by monitoring the uptake of either TF-A488 (5 μg/mL) or EGF-A488 (600 ng/mL) in COS7 and HER14 cells by fluorescence microscopy. The nuclei were stained with DAPI (shown as nuclear outlines) to indicate the position of the cells. (B) Quantitative analysis by high content screening of the effect of Pyrimidyn treatment on the CME of EGF-A488 in COS7 cells. Data are shown as a proportion of the DMSO-treated control. IC_{50} values are also shown (±95% CI, n = 2). (C) To investigate whether the effect of the Pyrimidyn compounds is reversible, cells were first incubated in 8 μM Pyrimidyn **6** or **7**, after which time the cells were washed and CME was assessed after a fixed 5 or 60 min. (D) Quantification of CME across a range of washout time points for Pyrimidyn **6**, showing that as washout time increases, the inhibitory effect of the compound diminishes. Error bars represent SEM.

and D). Therefore Pyrimidyn **6** and **7** effectively block CME in a range of non-neuronal cells.

Pyrimidyn 6 and 7 Block Dynamin I PH Domain Localization to the Cell Plasma Membrane. The PH domain of dynamin binds to phospholipids, which is necessary for localization of dynamin to the plasma membrane and regulation of CME.[14] Therefore the effect of Pyrimidyn analogue treatment on the localization of dynamin to the plasma membrane in cells was investigated. Confocal microscopy showed that GFP-dynamin I-PH localizes to the cytoplasm and plasma membrane (Figure 5A). Treatment of cells with Pyrimidyn **6** or **7** (30 μM) abolished GFP-dynamin I-PH at the plasma membrane (Figure 5B and C), an effect not seen with the parent Pyrimidyn **1** (Figure 5D). These results show that Pyrimidyn analogues disrupt dynamin localization to the plasma membrane via the PH domain and implicate this mechanism in the blockade of CME. To confirm this, we performed similar experiments using the GFP-tagged PH domain of phospholipase C delta (GFP-PLCδ-PH).[37] Treatment of cells with Pyrimidyn **6** or **7**, but not **1**, inhibited GFP-

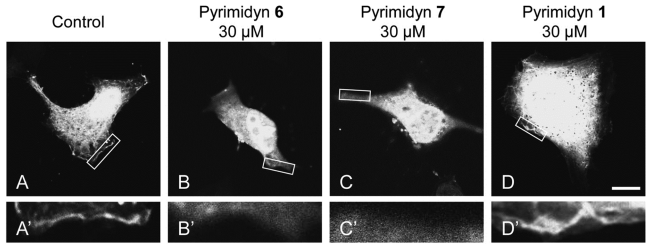

Figure 5. Pyrimidyn compounds prevent the localization of GFP-dyn I-PH domain to the plasma membrane. (A) HeLa cells were transfected with GFP-dyn I-PH domain, which localized to the cytosol and plasma membrane (see lower panel A' for detail). Pretreatment with Pyrimidyn **6** (B) or Pyrimidyn **7** (C) prevented the construct from localizing to the plasma membrane (shown in detail in the lower panels). This effect was not observed when cells were treated with Pyrimidyn **1** (D). Boxed regions indicate areas of the plasma membrane that are shown at higher magnification in the lower panels (A'–D'). Images are representative of two independent experiments. Scale bar =10 μM.

PLCδ-PH localization to the plasma membrane (Supplementary Figure S2) as previously reported for MiTMAB.[37]

Pyrimidyn Compounds Inhibit Synaptic Vesicle Turnover at Presynaptic Terminals. Neurotransmitter release during continuous or repeated synaptic depolarization is maintained by exocytosis and compensatory SVE at the presynaptic terminal. To examine the effects of **7** on SVE, a synaptic vesicle (SV) turnover assay was performed in synaptosomes. The styryl dye FM2-10 was used to label SVs as they undergo SVE, which is evoked by a first depolarization (S1). The amount of fluorescent labeling within the synaptosomes is measured in real time, and then the synaptosomes are challenged with a second depolarization (S2), evoking exocytosis of the dye-loaded SVs and resulting in a loss of fluorescence (Figure 6). When Pyrimidyn **7** (30 μM) was present during the dye loading step, a large inhibition of the amount of dye released by the second was observed (24.2 ± 10.9% of control, Figure 6A), which may indicate an inhibition of SVE. However, it is possible that **7** caused a defect in exocytosis and that this exocytic block could explain the lack of dye release from **7**-treated synaptic terminals. Therefore, its effect on exocytosis was investigated by measuring stimulated glutamate release from synaptosomes. Synaptosomes were incubated with Pyrimidyn **7** (30 μM) for 10 min and then depolarized using elevated KCl. The compound inhibited Ca^{2+}-dependent glutamate release by approximately 40% (58.6 ± 6.5% of control, Figure 6B). The mechanism behind this reduction in exocytosis observed after treatment with **7** is unclear.

To resolve whether the decrease in dye loading shown in Figure 6A could be explained solely by a smaller decrease in exocytosis, the retrieval efficiency was calculated.[11,48] FM2-10 dye loading was normalized to the total amount of glutamate release for each experimental condition. Under control conditions, the retrieval efficiency is 1, indicating that the amount of exocytosis is balanced by SVE. Values <1 indicate an inhibition of SVE, independent of the total amount of glutamate release by exocytosis. In synaptosomes treated with Pyrimidyn **7**, the retrieval efficiency was 0.41 ± 0.09 (Figure 6C), indicating a blockade in SVE independent of the compound's effect on exocytosis. It is possible that **7** may block a downstream SV trafficking event rather than SVE, since the SV turnover assay is dependent on SVs not only

dx.doi.org/10.1021/cb400137p | ACS Chem. Biol. 2013, 8, 1507–1518

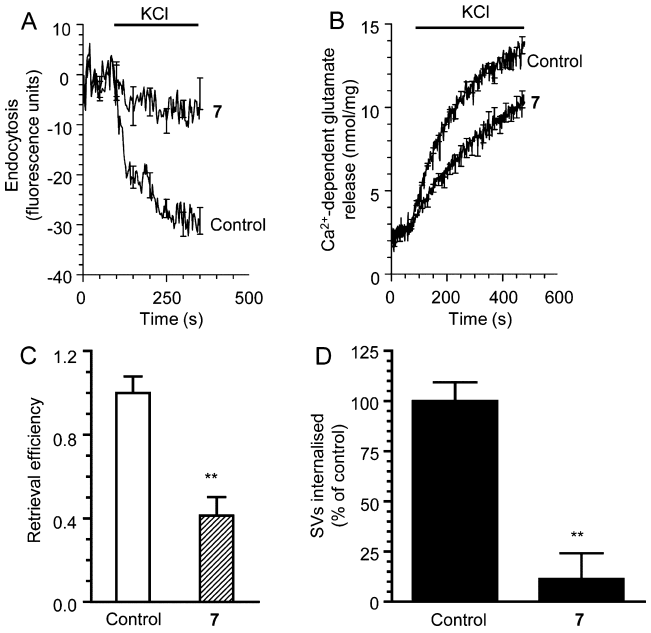

Figure 6. Pyrimidyn 7 inhibits SVE in rat brain synaptosomes. (A) Synaptosomes were incubated with DMSO or Pyrimidyn 7 (30 μM) for 10 min and then labeled with FM2-10 using a 2 min KCl stimulus. The amount of FM2-10 loaded into recycling SVs was then estimated with a subsequent unloading stimulus to release the accumulated dye. Endocytosis (calcium-dependent uptake and release of FM2-10) in the absence or presence of Pyrimidyn 7 is shown as the decrease in fluorescence. (B) To examine exocytosis, synaptosomes were preincubated with Pyrimidyn 7 (30 μM) for 10 min prior to stimulation with 30 mM KCl. The effect on SV exocytosis (calcium-dependent glutamate release) is displayed in the absence (control) or presence of Pyrimidyn 7. Period of KCl stimulation is indicated by the bar. (C) To determine the effect of Pyrimidyn 7 specifically on SVE, independent of any effect on exocytosis, the retrieval efficiency was calculated by dividing the values for FM2-10 uptake by the amount of exocytic glutamate release observed. Retrieval efficiency is expressed as a proportion of control. (D) Synaptosomes were loaded with FM2-10 as in panel A and then hypotonically lysed. Synaptic vesicles were purified and their Ca^{2+}-dependent FM2-10 labeling was quantified. Data are shown as a proportion of an untreated control. ** represents $P < 0.01$, Student's t test. $n = 3$ for all experiments. Scale bars represent SEM.

undergoing initial SVE during the S1 loading phase but also subsequently recycling into the releasable vesicle pool and exocytosis during the S2 phase. To demonstrate directly that 7 specifically arrested SVE, synaptosomes were depolarized in the presence of FM2-10 to facilitate dye uptake and immediately lysed, and SVs were isolated. The dye content of these SVs was then directly assessed by fluorometry, as described previously.[11] Treatment with Pyrimidyn 7 (30 μM) resulted in a nearly 90% decrease in FM2-10-labeling (11.3 ± 12.9% of control, Figure 6D), suggesting a specific arrest in the generation of new SVs by SVE. To determine an IC_{50} for the inhibition of SVE, we used a high throughput SVE assay, yielding IC_{50} values of 10.7 ± 3.1 μM for Pyrimidyn **6** and 9.7 ± 2.5 μM for Pyrimidyn 7 (Supplementary Table S1). Overall, these observations demonstrate that Pyrimidyn **6** and 7 potently inhibit SVE in synaptic terminals, presumably through inhibition of dynamin I.

Pyrimidyns Inhibit Proliferation and Induce Cell Death in Cancer Cells. In addition to its role in CME, dynamin is essential for cytokinesis, the final step of cell division. The dynamin inhibitors MiTMAB and Dynole 34-2 have antimitotic properties that preferentially target cancer cells, causing them to undergo apoptosis.[50,62,63] We therefore investigated the effects of Pyrimidyn **6** and 7 in HeLa cells with regards to toxicity, cell death, and proliferation.

The acute cellular toxicity of the compounds was analyzed first. After 8 h of treatment, **6** and 7 exhibited significant toxicity at concentrations of 30 and 100 μM, using an LDH release assay (Figure 7A). The LDH assay does not discriminate between cell death by necrosis or apoptosis; however, given the short time frame of the treatment it is unlikely that there was significant necrosis. To further investigate whether Pyrimidyn compounds could induce apoptosis, the drug incubation time was increased from 8 to 20 h for trypan blue and DNA fragmentation assays, which indicate cell apoptosis. Both Pyrimidyns reduced cell viability as measured by trypan blue uptake at concentrations of 10 and 30 μM. At these concentrations, Pyrimidyn **6** induced a small increase in DNA fragmentation, while Pyrimidyn 7 greatly increased fragmentation, indicating apoptosis. It is notable that at 10 μM, Pyrimidyn **6** induced no significant increase in LDH release after 8 h but at 20 h greatly increased trypan blue-positive cells and DNA fragmentation (assessed using flow cytometry analysis of propidium iodide uptake), suggesting that at relatively low concentrations these compounds can induce apoptosis in HeLa cells. These findings suggest that although Pyrimidyns exhibit nonspecific cytotoxicity at relatively high concentrations, at lower concentrations they are able to induce cell death through apoptosis.

MiTMAB and Dynole 34-2 have both been shown previously to inhibit cell proliferation, due to the requirement for dynamin function in cytokinesis. The growth inhibitory properties of Pyrimidyns **6** and 7 were examined in a panel of cancer cell lines for 72 h. Both compounds potently inhibited growth of all cell lines tested, exhibiting GI_{50} values for Pyrimidyn **6** from 0.8 to 2.5 μM and for Pyrimidyn 7 from 1.3 to 3.2 μM. Collectively, these findings suggest that while the Pyrimidyn analogues may have some acute cytotoxic effects at relatively high concentrations, at lower concentrations they exhibit favorable anticancer properties.

Discussion. We report the design of a novel family of dynamin inhibitors, called the Pyrimidyn series, a name that reflects that the family was based on their core pyrimidine structure. These compounds are the first dynamin inhibitors with a defined dual mechanism of action. Kinetic analysis of GTPase activity showed that Pyrimidyn compounds interfere with the binding of dynamin to GTP, thereby preventing GTP hydrolysis. In addition, Pyrimidyns competitively prevent dynamin from binding to lipid. This lipid-competitive activity is likely the result of some structural similarities between the Pyrimidyn analogues and the long chain amine dynamin inhibitors, such as MiTMAB, which also act at the PH domain to prevent lipid binding. Pyrimidyns inhibit basal activity of dynamin, as demonstrated by their ability to inhibit GTPase activity of the dynamin GTPase-GED construct. This construct lacks a PH domain or ability to oligomerize beyond a dimer, supporting the dual mechanism of action.

The development of the Pyrimidyn series focused on substituted pyrimidines that are known to act as nucleotide mimics,[38−40] an appealing structure due to the potential to competitively bind to the GTP binding site of dynamin. Initial library screening identified Pyrimidyn **1** (Supplementary Table S1, **1**) as a 37.8 ± 9.4 μM inhibitor, which then served as the parent compound for a subsequent series. Production of

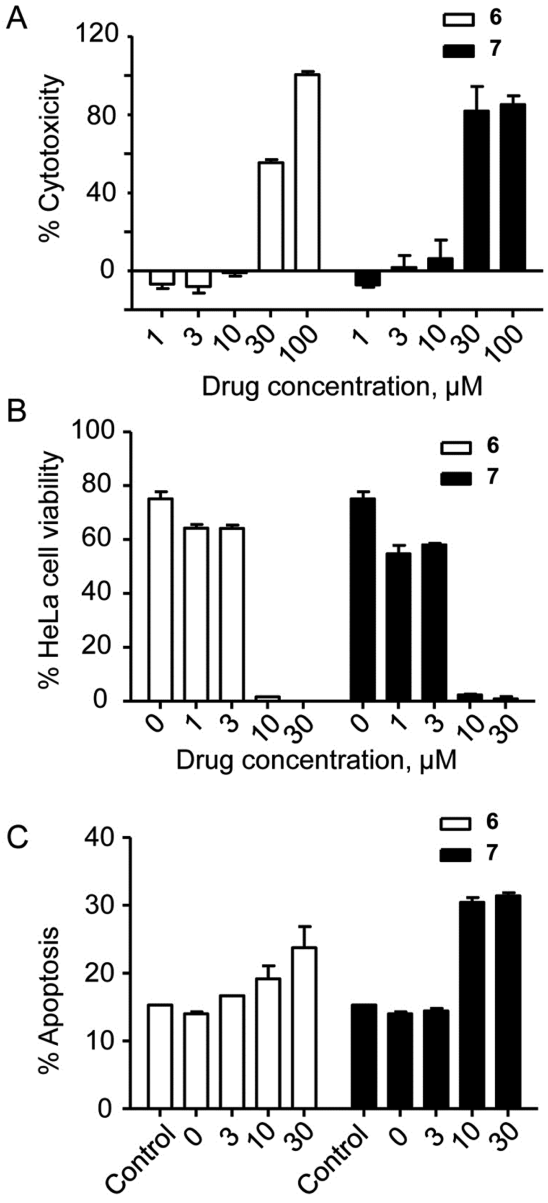

D

Pyrimidyn	HT29 [a]	SW480 [a]	MCF-7 [b]	A2780 [c]	H460 [d]	A431 [e]	DU145 [f]	BE2-C [g]	SJ-G2 [h]	U87 [h]	MIA PaCa2 [i]	SMA [j]
6	1.4 ± 0.1	0.8 ± 0.03	1.5 ± 0.0	1.8 ± 0.5	2.5 ± 0.2	1.7 ± 0.2	1.9 ± 0.1	1.5 ± 0.0	1.5 ± 0.0	1.5 ± 0.0	1.5 ± 0.0	1.3 ± 0.2
7	1.3 ± 0.2	1.3 ± 0.2	1.4 ± 0.2	1.3 ± 0.2	1.6 ± 0.0	2.4 ± 0.4	3.2 ± 0.1	1.4 ± 0.1	1.5 ± 0.0	1.5 ± 0.0	1.5 ± 0.0	1.4 ± 0.2

[a] HT29 and SW480 (colon carcinoma), [b] MCF-7 (breast carcinoma), [c] A2780 (ovarian carcinoma), [d] H460 (lung carcinoma), [e] A431(skin carcinoma), [f] DU145 (prostate carcinoma), [g] BEC-2 (neuroblastoma), [h] SJ-G2 and U87 (glioblastoma), [i] MIA PaCa2 (pancreatic carcinoma); [j] SMA (spontaneous murine astrocytoma).

Figure 7. Cellular toxicity and growth inhibition induced by Pyrimidyn **6** and **7**. (A) LDH measurement for general cytotoxicity was performed at 8 h after drug treatment on asynchronously growing HeLa cells. Values were normalized to drug/media background value, and toxicity was calculated as a percentage of a 100% lysed cell control. (B) Trypan blue measurement of membrane integrity. Hela cells were treated in the presence or absence of the dynamin inhibitor at indicated concentrations, and after 20 h the cell number and viability were measured. (C) FACS analysis quantitation of sub-G1 peak − measures apoptosis as indicated by DNA fragmentation. HeLa cells were treated in the presence or absence of the dynamin inhibitor at indicated concentrations and after 20 h were collected, fixed, and stained with propidium iodide, and the cell cycle was analyzed. (D) Growth inhibition (GI_{50}, μM) was examined in a panel of cancer cell lines using the MTT growth inhibition assay after 72 h of continuous exposure to Pyrimidyn **6** and **7**.

regioisomers **2** and **3** containing a 2-dimethylaminoethyl group (Figure 1, **2** and **3**) increased the potency (Supplementary Table S1). Addition of a *N*-dodecyl side chain (**5**), resulting in structures similar to the long chain amine dynamin inhibitors,[28,37] gave potency similar to that of the lead compound (Figure 1, **5**). Hybridization of **5** and **2**/**3**, creating

dx.doi.org/10.1021/cb400137p | *ACS Chem. Biol.* 2013, 8, 1507−1518

compounds with both an *N*-dodecyl side chain and a 2-dimethylaminoethyl group, produced **6** and **7** (Figure 1: **6** and **7**), the most potent compounds of the series (Supplementary Table S1).

Dynamin is an attractive target for the development of small molecule inhibitors. First, it is involved in a number of cellular processes, not only being essential in many forms of endocytosis, but also involved in cytokinesis and regulating actin dynamics.[4,64] Second, dynamin has a number of unique structural and functional qualities that limit the chances of creating inhibitors that also interfere with other proteins involved in endocytosis.[6] Third, endocytosis is easily amenable to high content screening strategies.[49] Finally, dynamin activity can be rapidly assayed using a simple GTPase assay, necessary for compound screening.[43] This assay has allowed us to identify several series of dynamin inhibitors, all with distinct structures and mechanisms of action.[27,49] While Pthaladyn compounds are GTP-competitive and RTILs/long chain amines are lipid-competitive, Pyrimidyn compounds are the first to exhibit both mechanisms of action. Pthaladyns allow the involvement of GTP hydrolysis by dynamin in a given process to be investigated without any effects on dynamin recruitment to lipid membranes. Pthaladyns will also inhibit the activity of GTP hydrolysis that occurs in the absence of lipid. RTILs and long chain amines like MiTMAB, by contrast, allow the specific inhibition of dynamin binding to lipid, leaving GTP hydrolysis unaffected. In a cellular context, this would prevent dynamin involvement in endocytosis, which is dependent on lipid binding, but would leave the role of dynamin GTPase in other processes, such as actin dynamics, to be investigated. As the Pyrimidyns inhibit both GTP and lipid binding, they provide complete abolition of dynamin function. In particular, a compound that blocks dynamin function only at the membrane, such as MiTMAB, will not block dynamin's cytoplasmic functions in actin dynamics. Thus our new tools, in combination with use of other inhibitors, provide potential useful controls to tease out the subcellular compartment in which dynamin is functioning for a particular process. Together, the three classes of compound provide the pharmacological equivalent of having the GTPase domain (Pthaladyns), the PH domain (RTILs/long chain amines), or both domains (Pyrimidyns) deleted. Thus, the use of these compounds together provides a useful toolbox to dissect the role of different dynamin domains.

Dynamin II, which is also targeted by these compounds, is ubiquitously expressed and required for CME. Both **6** and **7** block the uptake of both EGF and Tf in a variety of non-neuronal cells, suggesting that these compounds can be used as inhibitors of dynamin-dependent endocytosis. The interaction between dynamin's PH domain and membrane phospholipids is essential in CME.[13,65] Pyrimidyn compounds disrupt the binding of dynamin to lipid *in vitro* and prevent the recruitment of dynamin I-PH-EGFP to the plasma membrane in cells. Thus, we propose that although Pyrimidyn compounds have a dual mechanism of action *in vitro*, they inhibit CME primarily by preventing the recruitment of dynamin to the plasma membrane, thereby inhibiting dynamin function prior to GTP binding and hydrolysis. This mechanism of action raises the possibility of off-target membrane actions of compounds in this category, such as observed with cationic amphiphilic drugs that inhibit endocytosis by unclear mechanisms.[25]

Dynamin I is primarily expressed in neurons, where it is involved in the regulation of SVE,[66,67] although it is also present in chromaffin cells[68] and mature sperm.[69] At 30 μM, Pyrimidyn **7** caused a partial reduction in Ca^{2+}-dependent exocytosis in synaptosomes. Although the molecular mechanism for this effect is unclear, one potential explanation relates to recent evidence suggesting a dynamin role in fusion pore stability in chromaffin cells, which also express dynamin I and II.[68,70] Alternatively, it may also result from the compounds' capacity to interact with lipid membranes. However, after treatment with Pyrimidyn **7** (30 μM), synaptosomes retain 60% of their normal exocytic capacity. After the reduction in exocytosis is taken into account, synaptosomes treated with Pyrimidyn **7** exhibit a 60% reduction in retrieval efficiency, which is a measure of SV recycling. Further investigation showed that treatment with **7** greatly reduced the uptake of FM2-10 by SVE, demonstrating that **7** is able to abolish SVE in synaptosomes. Given the essential role for dynamin I in SVE, it is likely that the reduction in SVE occurs through inhibition of dynamin. We postulate that this endocytic block is likely to be mediated through a failure by dynamin to be recruited to the plasma membrane due to the Pyrimidyn compounds' ability to competitively target the PH domain of dynamin.

The relatively low level of nonspecific cytotoxicity of Pyrimidyns **6** and **7** suggests that the compounds do not cause significant physical damage to cellular lipids unless relatively high concentrations are used. At lower concentrations, these Pyrimidyns induce a cell death pathway that is consistent with an apoptotic mechanism in HeLa cells. Further, the compounds potently induce growth arrest in 12 different cancer cell lines after treatment for 72 h. The compounds exhibited similar IC_{50} values across all cell lines, suggesting that a common mechanism is targeted. Recent studies have highlighted the possible utility of MiTMAB and Dynole 34-2 as potential antimitotic agents and have identified dynamin II as novel target for the treatment of cancer.[50,71] The effectiveness of the Pyrimidyns as inhibitors of cell proliferation at concentrations well below the threshold for induction of cytotoxicity suggests that the Pyrimidyns may present novel compounds for dynamin-targeted anticancer therapy. Further investigation will be informative regarding the extent to which cancer cells are specifically targeted.

In summary, we have developed and characterized a series of novel pyrimidine-based dynamin inhibitors. The Pyrimidyns are the first compounds described to have a dual mechanism of dynamin inhibition. The most active of the series, **6** and **7**, are able to enter a broad range of cells where they block dynamin-dependent functions in CME, SVE, and the growth of cancer cells. In combination with the existing palette of single-mechanism dynamin inhibitors, the Pyrimidyn analogues will be useful as tools in dissecting the role of dynamin in cellular function and potentially in treating diseases in which dynamin-dependent functions are implicated, such as cancer.

METHODS

Materials. For drug synthesis all starting materials were purchased from Sigma-Aldrich (St. Louis, MO, U.S.A.) and Lancaster Synthesis (Windham, NH, U.S.A.). All bulk solvents were distilled from glass prior to use. Phosphatidylserine (PS), phenylmethylsulfonylfluoride (PMSF), and Tween 80 were from Sigma-Aldrich. GTP was from either Sigma-Aldrich or Roche Applied Science (Basel, Switzerland), and leupeptin was from Bachem (Bubendorf, Switzerland). Gel electrophoresis reagents, equipment, and protein molecular weight markers were from Bio-Rad (Hercules, CA, U.S.A.). Collagenase was from Roche. Paraformaldehyde (PFA) was from BDH (AnalaR Merck Chemicals, Darmstadt, Germany). Phosphate buffered salts, fetal calf

serum (FCS), and Dulbecco's Minimal Essential Medium (DMEM) were from Invitrogen (Paisley, Strathclyde, U.K.). Texas-red conjugated transferrin (Tf-TxR), Alexa-488 conjugated EGF (EGF-A488), Alexa-594 conjugated Tf (Tf-A594), DAPI, and FM-2-10 were from Molecular Probes (Eugene, OR, U.S.A). All other reagents were of analytical reagent grade or better.

Pyrimidyn, MiTMAB, Dynole, Iminodyn, Pthaladyn, Dyngo, and Rhodadyn are trademarks of Children's Medical Research Institute and Newcastle Innovation Ltd. and are available from Abcam Biochemicals Ltd. (Bristol, U.K.).

Preparation of Compounds for Testing. All compounds were prepared in 100% dimethylsulfoxide (DMSO), generally at 30 mM concentration and stored at −20 °C for several months. For the GTPase assay, compound stocks were diluted in 10% DMSO made up in 20 mM Tris/HCl pH 7.4, then again diluted into the final assay (final DMSO concentration of 1%). The GTPase assay for dynamin I or II was unaffected by DMSO up to 1%. Endocytosis assays were also performed with a final DMSO concentration of 1%.

Protein Production. Dynamin I was purified from sheep brain by extraction from the peripheral membrane fraction of whole brain[41] and affinity purification on GST-Amph2-SH3-sepharose as described,[42,43] yielding 8−10 mg protein from 250 g of sheep brain. GTPase-GED, a truncated version of dynamin I containing GTPase and GED domains,[44] plasmid construct was expressed in *E. coli*. Dynamin II was purified as previously described.[30,32] In brief, dynamin II (His-6-tagged) DNA was inserted in to the pIEx-6 vector, and the plasmid was used to transfect Sf21 insect cells using polyethylenimine as the transfection reagent using a DNA/polyethylenimine ratio of 1:5 for 48 h.[45] Following transfection the cells were harvested, and dynamin II purified using GST-Amph2-SH3-sepharose. The yield from 1 L of insect cell suspension culture (1×10^6 cells/mL) was typically 9 mg protein with greater than 98% purity.

Dynamin GTPase Assay. The Malachite Green method was used for the sensitive colorimetric detection of orthophosphate (P_i) release from GTP as previously described.[30,32] Dynamin I and II activity was stimulated by sonicated phosphatidylserine (PS) liposomes. Data analysis and enzyme kinetics using nonlinear regression was performed using GraphPad Prism (GraphPad Software Inc., San Diego, CA). The curves were generated using the Michaelis−Menten equation: $v = V_{max}[S]/(K_m + [S])$, where S = PS activator or GTP substrate. After the V_{max} and K_m values were determined, the data was transformed using the Lineweaver−Burke equation: $1/v = 1/V_{max} + (K_m/V_{max})*(1/[S])$. GTPase-GED activity was detected as orthophosphate (P_i) released from GTP using Malachite Green as a P_i chelator. Purified GTPase-GED (2000 nM) was incubated in GTPase assay buffer (5 mM Tris-HCl, 10 mM NaCl, 2 mM Mg^{2+}, 0.05% Tween-80, pH 7.4 plus 1 μg/mL leupeptin, and 0.1 mM PMSF) with 0.5 mM GTP in the presence of Pyrimidyns at 37 °C for 60 min.

Phospholipid Binding. Dynamin I (20 nM) was incubated with sonicated PS liposomes (100 μM) in 100 μL of assembly buffer (1 mM EGTA, 30 mM Tris, 100 mM NaCl, 1 mM DTT, 1 mM PMSF, and Roche Complete protease inhibitor cocktail, 1 tablet per 50 mL) for 30 min at RT (22 °C). Samples were then centrifuged at 14,000*g* for 15 min to separate lipid-bound and free dynamin. Fractions were analyzed by gel electrophoresis on a 12% SDS polyacrylamide gel followed by staining with Coomassie Brilliant Blue.

CME Assay. CME was examined by quantifying the uptake of Texas Red-conjugated human transferrin (Tf-TxR) or Alexa-488-conjugated EGF (EGF-A488) in either COS-7 or HER14 cells, based on methods described previously.[46,46] Briefly, cells were maintained in DMEM supplemented with 10% fetal bovine serum and incubated at 37 °C in 5% CO_2. For qualitative imaging, cells were plated on glass coverslips to 60% confluency and then serum-starved overnight (16 h) in DMEM minus fetal bovine serum. Cells were then preincubated with drugs or vehicle (1% DMSO) for 10 or 15 min prior to addition of 5 μg/mL Tf-TxR or 1 μg/mL EGF-A488 for 10 min at 37 °C. Cell surface-bound Tf or EGF was removed by incubating the cells in an ice-cold acid wash solution (0.2 M acetic acid + 0.5 M NaCl, pH 2.8) for 15 min followed by an ice-cold PBS wash for 5 min. Cells were immediately fixed with 4% PFA for 10 min and washed 3 times with PBS at RT. Nuclei were stained using DAPI. Coverslips were mounted using mounting medium containing DABCO, and the fluorescence was monitored using a Leica DMLB bright field microscope and SPOT digital camera.

Quantitative analysis of EGF-A488 uptake in COS7 cells was performed by high content imaging. COS-7 cells were grown in poly-D-lysine-coated 96-well plates, and EGF-A488 uptake was preformed as described above, except that cells were washed twice in cold PBS prior to the acid wash step. All conditions were carried out in triplicate. Green (EGF-A488) and blue (DAPI) images were collected automatically using an Olympus IX81 epifluorescence microscope. Nine images were collected from each well, averaging 40−50 cells per image. The average integrated intensity of EGF-A488 signal per cell was calculated for each well using Metamorph (Molecular Devices), and the data were expressed as a percentage of control cells (vehicle treated only). The average number of cells for each data point was ∼1200. IC_{50} values were calculated using Graphpad Prism, and data were expressed as mean 95% confidence interval (CI) for 3 wells and ∼1,200 cells.

EGFR Activation and Western Blot Analysis. A431 cells were cultured in 100 mm dishes to 80% confluency followed by serum starvation overnight (16 h) in DMEM minus serum. Cells were then incubated with Pyrimidyn 7 (30 μM), DMSO (vehicle control), or Genistein (30 μM; negative control) for 10 min prior to addition of unconjugated EGF (100 ng/mL) for 10 min at 37 °C. All conditions were carried out in duplicate. After 10 min incubation, cells were placed on ice and washed 4 times with ice cold PBS. Total cell lysates were prepared by incubating cells for 10 min with lysis buffer (20 mM Tris/HCl pH 7.4, 2 mM EDTA, 2 mM EGTA, 1% TritonX-100, 10 μg/mL leupeptin, 1 mM PMSF, Complete protease inhibitor tablet (Roche), 2 mM imidazole, 1 mM sodium fluoride, 2 mM sodium orthovanadate, 1 mM sodium molybdate, 4 mM sodium tartrate dihydrate). The mixture was then centrifuged at 14,000*g* for 10 min, and supernatant was harvested as the total cell lysate. Fifty micrograms of total cell lysate for each condition was resolved on a 12% SDS-polyacrylamide gel and then transferred onto Protran immobilized nitrocellulose membrane (PerkinElmer). The membranes were probed with mouse anti-phosphotyrosine PY20 monoclonal antibody (BD Biosciences, San Jose, CA). The secondary antibody was goat anti-mouse polyclonal antibody conjugated to HRP (Dako, Denmark), and signal was developed with SuperSignal West Pico chemiluminescence (Pierce Chemical). The membranes were stripped with 0.2 M NaOH, reprobed for endogenous EGFR using mouse anti-EGFR 1F4 monoclonal antibody (Cell Signaling Technology, Danvers, MA), and developed as above. Western blots were scanned using the BioRad GS800 Densitometer (BioRad, Hercules, CA), and densitometry analysis was performed by Quantity One software (BioRad). EGFR phosphotyrosine (pEGFR) signal was normalized against total EGFR signal and expressed as relative intensity (%) of the stimulated control (DMSO) condition, and the average of range of values ($n = 2$) was plotted.

PH Domain Localization in Cells. The cDNA of the PH domain of dynamin I (rat sequence, amino acids Thr-511 to Lys-635) was cloned by PCR and recombination into the GATEWAY entry vector pDONR201 (Invitrogen). The cDNA was subcloned by recombination into pcDNA-DEST53 (mammalian N-terminal GFP-tag) expression vector (Invitrogen). HeLa cells were plated on glass coverslips and transfected with 0.2 μg of GFP-dyn 1-PH or GFP-PLCδ-PH DNA per well (24 wells/550 μL final volume/well) using FuGENE according to the manufacturer's instructions and analyzed 48 h after transfection. Cells were serum starved for 2 h at 37 °C, after which they were treated with 30 μM concentration of the Pyrimidyn compound for 10 min. Cells were incubated for a further 20 min in the presence of Tf-A594 or EGF-TxR, first as internal positive controls that the drugs worked and second, that expression of the construct did not inhibit endocytosis (data not shown). Cells were then fixed with 3% PFA in PBS. The distribution of GFP-dyn 1-PH, GFP-PLCδ-PH, and Tf-A594 or EGF-TxR was determined by fluorescence microscopy. Optical sections were analyzed by confocal laser scanning

microscopy using a Leica TCS SP2 system (Leica Microsystems, Heidelberg, Germany).

Glutamate Release Assay. Synaptosomes were prepared from rat cerebral cortex by centrifugation on discontinuous Percoll gradients.[47] The glutamate release assay was performed as described previously.[48] Briefly, synaptosomes (0.6 mg in 2 mL) were resuspended in either plus (1.2 mM $CaCl_2$) or minus (1 mM EGTA) Ca^{2+} Krebs-like solution (118.5 mM NaCl, 4.7 mM KCl, 1.18 mM $MgCl_2$, 0.1 mM Na_2HPO_4, 20 mM Hepes, 10 mM glucose, pH 7.4) at 37 °C. Experiments were initiated after the addition of 1 mM $NADP^+$ and after 1 min the addition of glutamate dehydrogenase (50 U). The synaptosome suspension was stimulated after 4 min with 30 mM KCl. Increases in fluorescence due to production of NADPH were monitored in a spectrofluorimeter at excitation of 340 nm and emission at 460 nm. Experiments were standardized by the addition of 4 nmol of glutamate. Data are presented as Ca^{2+}-dependent glutamate release, calculated as the difference between release in plus and minus Ca^{2+} solution for identical stimulation conditions. Where indicated synaptosomes were preincubated with Pyrimidyn 7 for 10 min before and during stimulation.

SV Turnover Assay. SV turnover was measured using uptake of the fluorescent dye FM2-10 as previously described.[48] Synaptosomes (0.6 mg in 2 mL) were incubated for 5 min at 37 °C in plus or minus Ca^{2+} Krebs-like solution. FM2-10 (100 μM) was added 1 min before stimulation with 30 mM KCl (S1). After 2 min of stimulation, synaptosomes were washed twice in plus Ca^{2+} solution supplemented with 1 mg/mL bovine serum albumin. Synaptosomes were then resuspended in plus Ca^{2+} solution at 37 °C, transferred to a fluorimeter cuvette, and stimulated with a standard addition of 30 mM KCl (S2). The extent of SV turnover was estimated as the decrease in FM2-10 fluorescence due to dye release into solution (excitation 488 nm, emission 540 nm). The displayed traces represent the release of FM2-10 from synaptosomes after subtraction of background traces acquired from synaptosomes loaded with FM2-10 in the absence of Ca^{2+}. Retrieval efficiency was calculated as SV turnover/SV exocytosis (as determined using the glutamate release assay described above), where SV turnover is defined as the number of SV recycled by endocytosis and exocytosis as Ca^{2+}-dependent glutamate release after 7 min of KCl stimulation. Pyrimidyn 7 was added for 10 min before and during S1 loading where indicated.

SV Internalization Assay. The SV internalization assay was performed as described previously.[11] Synaptosomes were loaded with 100 μM FM2-10 and washed in an identical manner as in the SV turnover assay. The synaptosomes were hypotonically lysed by resuspension and vortexing in 20 mM Tris, pH 7.4, for 10 s and supplemented with KCl to 150 mM. The lysed synaptosomes were centrifuged at 14,000 rpm for 2 min in a microfuge, the supernatant (containing SVs) was collected, and the fluorescence was measured at 488 nm excitation and 540 nm emission. The amount of internalized FM2-10 was calculated by subtracting the fluorescence in plus from minus Ca^{2+} solutions.

High Throughput SVE Assay. The high throughput SVE assay was performed using purified synaptosomes from the brains of adult male Wistar rats, as previously described.[49] Experiments were performed in 96-well microplates, using triplicate wells for each treatment condition.

Cell Culture (For Cytotoxicity Assays). HeLa and H460 cells were maintained in RPMI 1640 medium supplemented with 10% fetal bovine serum and 5% penicillin/streptomycin (P/S). All other cell lines were maintained in Dulbecco's modified Eagle's media (DMEM) supplemented with 10% serum and 5% P/S. All cells were grown at 37 °C in a humidified 5% CO_2 atmosphere.

Lactate Dehydrogenase (LDH) Toxicity Assay. Toxicity was assayed by determination of LDH activity. HeLa cells were seeded in 96-well plates. Asynchronously growing cells were treated in the presence or absence of the dynamin inhibitor at the indicated concentration for 8 h. The supernatant (50 μL) was added to 100 μL of LDH assay reagent (Sigma-Aldrich), and the reaction was allowed to developed for 20 min. Absorbance was measured at 490 and 690 nm (plate background absorbance). Values were normalized to drug/media background value, and toxicity was calculated as a percent of a 100% lysed cell control.

Trypan Blue Exclusion Assay. Cells were seeded in 10 cm^2 dishes (1×10^5 cells/dish). On day 0 (24 h after seeding), cells in triplicate were treated in the presence or absence of the dynamin inhibitor at concentrations of 1, 3, 10, and 30 μM. After 20 h, the cell number and viability were measured using a Vi-CELL XR cell viability analyzer as previously described.[50]

Cell Cycle Analysis by Flow Cytometry. Cells (5×10^5) were grown in 10 cm dishes. Following inhibitor treatment, cells (floating and adherent) were collected, and single-cell suspensions were fixed in 80% ice-cold ethanol at −20 °C for at least 16 h. Cells were stained with propidium iodide, and the cell cycle was analyzed as described previously.[50] Cell cycle profiles were acquired with a FACS Canto Flow Cytometer (Becton Dickinson) using FACS Diva software (v5.0.1) at 488 nm. Cell cycle profiles were analyzed using FlowJo software (v7.1).

***In Vitro* Growth Inhibition Assay (MTT Assay).** Growth inhibitory assays were carried out as described previously described.[51] A 30 mM stock solution of each test compound was prepared in dimethylsulfoxide (DMSO) and stored at −20 °C. All cell lines were cultured at 37 °C under 5% CO_2 in air and were maintained in Dulbecco's modified Eagle's medium (Trace Biosciences, Australia) supplemented with 10% fetal bovine serum, 10 mM sodium bicarbonate penicillin (100 IU/mL), streptomycin (100 μg/mL), and glutamine (4 mM). Cells in logarithmic growth were transferred to 96-well plates. Growth inhibition was determined by plating cells in duplicate in 100 mL of medium at a density of 2,500−4,000 cells/well. On day 0 (24 h after plating), when the cells were in logarithmic growth, 100 μL of medium with or without the test agent was added to each well. After 72 h of drug exposure growth inhibitory effects were evaluated using the MTT (3-[4,5-dimethyltiazol-2-yl]-2,5-diphenyltetrazolium bromide) assay, and absorbance was read at 540 nm. A dose−response curve was produced allowing for the calculation of a GI_{50} value, which is the drug concentration (μM) that inhibits cell growth by 50% based on the difference between the optical density values on day 0 and those at the end of drug exposure. Each value is the mean ± SEM of three independent analyses.

■ ASSOCIATED CONTENT

Ⓢ Supporting Information

This material is available free of charge *via* the Internet. http://pubs.acs.org/journal/acbcct

■ AUTHOR INFORMATION

Corresponding Author

*E-mail: probinson@cmri.org.au.

Present Address

○Neuroscience Research Australia Hospital Road, Randwick NSW 2031, Australia (A.B.M.). Organic Pharmaceutical Chemistry, Department of Medicinal Chemistry, Uppsala Biomedical Centre, Uppsala University, Box 574, SE-751 23 Uppsala, Sweden (L.R.O.). Division of Chemistry and Structural Biology, Institute for Molecular Bioscience, University of Queensland, Brisbane, Queensland 4072 (T.A.H.).

Author Contributions

#These authors contributed equally to this work.

Notes

The authors declare no competing financial interest.

■ ACKNOWLEDGMENTS

This work was supported by grants and Fellowships from the National Health and Medical Research Council (Australia) to P.J.R. and A.M. and The Wellcome Trust (ref. 062841). We thank J. Chappie and S. Schmid for the GTPase-GED plasmid constructs. We thank the Ramaciotti Foundation, the Ian Potter

Foundation, the Australian Cancer Research Foundation and the Cancer Institute of New South Wales for financial support. D.J.K. was supported by the TM Ramsay Fellowship.

REFERENCES

(1) McMahon, H. T., and Boucrot, E. (2011) Molecular mechanism and physiological functions of clathrin-mediated endocytosis. *Nat. Rev. Mol. Cell. Biol. 12*, 517−533.
(2) Liu, J. P., and Robinson, P. J. (1995) Dynamin and endocytosis. *Endocr. Rev. 16*, 590−607.
(3) Conner, S. D., and Schmid, S. L. (2003) Regulated portals of entry into the cell. *Nature 422*, 37−44.
(4) Ferguson, S. M., and De Camilli, P. (2012) Dynamin, a membrane-remodelling GTPase. *Nat. Rev. Mol. Cell. Biol. 11*, 75−88.
(5) Hinshaw, J. E. (2000) Dynamin and its role in membrane fission. *Annu. Rev. Cell Dev. Biol. 16*, 483−519.
(6) Cousin, M. A., and Robinson, P. J. (2001) The dephosphins: Dephosphorylation by calcineurin triggers synaptic vesicle endocytosis. *Trends Neurosci. 24*, 659−665.
(7) Muhlberg, A. B., Warnock, D. E., and Schmid, S. L. (1997) Domain structure and intramolecular regulation of dynamin GTPase. *EMBO J. 16*, 6676−6683.
(8) Sever, S., Muhlberg, A. B., and Schmid, S. L. (1999) Impairment of dynamin's GAP domain stimulates receptor-mediated endocytosis. *Nature 398*, 481−486.
(9) Scaife, R., Venien-Bryan, C., and Margolis, R. L. (1998) Dual function C-terminal domain of dynamin-1: modulation of self-assembly by interaction of the assembly site with SH3 domains. *Biochemistry 37*, 17673−17679.
(10) Graham, M. E., Anggono, V., Bache, N., Larsen, M. R., Craft, G. E., and Robinson, P. J. (2007) The in vivo phosphorylation sites of rat brain dynamin I. *J. Biol. Chem. 282*, 14695−14707.
(11) Anggono, V., Smillie, K. J., Graham, M. E., Valova, V. A., Cousin, M. A., and Robinson, P. J. (2006) Syndapin I is the phosphorylation-regulated dynamin I partner in synaptic vesicle endocytosis. *Nat. Neurosci. 9*, 752−760.
(12) Praefcke, G. J., and McMahon, H. T. (2004) The dynamin superfamily: universal membrane tubulation and fission molecules? *Nat. Rev. Mol. Cell. Biol. 5*, 133−147.
(13) Vallis, Y., Wigge, P., Marks, B., Evans, P. R., and McMahon, H. T. (1999) Importance of the pleckstrin homology domain of dynamin in clathrin-mediated endocytosis. *Curr. Biol. 9*, 257−260.
(14) Achiriloaie, M., Barylko, B., and Albanesi, J. P. (1999) Essential role of the dynamin pleckstrin homology domain in receptor-mediated endocytosis. *Mol. Cell. Biol. 19*, 1410−1415.
(15) Ramachandran, R., Pucadyil, T. J., Liu, Y. W., Acharya, S., Leonard, M., Lukiyanchuk, V., and Schmid, S. L. (2009) Membrane insertion of the pleckstrin homology domain variable loop 1 is critical for dynamin-catalyzed vesicle scission. *Mol. Biol. Cell 20*, 4630−4639.
(16) Roux, A., Uyhazi, K., Frost, A., and De Camilli, P. (2006) GTP-dependent twisting of dynamin implicates constriction and tension in membrane fission. *Nature 441*, 528−531.
(17) Marks, B., Stowell, M. H., Vallis, Y., Mills, I. G., Gibson, A., Hopkins, C. R., and McMahon, H. T. (2001) GTPase activity of dynamin and resulting conformation change are essential for endocytosis. *Nature 410*, 231−235.
(18) Morlot, S., Galli, V., Klein, M., Chiaruttini, N., Manzi, J., Humbert, F., Dinis, L., Lenz, M., Cappello, G., and Roux, A. (2012) Membrane shape at the edge of the dynamin helix sets location and duration of the fission reaction. *Cell 151*, 619−629.
(19) Ivanov, A. I. (2008) Pharmacological inhibition of endocytic pathways: is it specific enough to be useful? *Methods Mol. Biol. 440*, 15−33.
(20) Atwood, W. J. (2001) A combination of low-dose chlorpromazine and neutralizing antibodies inhibits the spread of JC virus (JCV) in a tissue culture model: Implications for prophylactic and therapeutic treatment of progressive multifocal leukencephalopathy. *J. Neurovirol. 7*, 307−310.
(21) Gray, J. A., Sheffler, D. J., Bhatnagar, A., Woods, J. A., Hufeisen, S. J., Benovic, J. L., and Roth, B. L. (2001) Cell-type specific effects of endocytosis inhibitors on 5-hydroxytryptamine2A receptor desensitization and resensitization reveal an arrestin-, GRK2-, and GRK5-independent mode of regulation in human embryonic kidney 293 cells. *Mol. Pharmacol. 60*, 1020−1030.
(22) Davies, P. J., Cornwell, M. M., Johnson, J. D., Reggianni, A., Myers, M., and Murtaugh, M. P. (1984) Studies on the effects of dansylcadaverine and related compounds on receptor-mediated endocytosis in cultured cells. *Diabetes Care 7* (Suppl 1), 35−41.
(23) Larkin, J. M., Brown, M. S., Goldstein, J. L., and Anderson, R. G. (1983) Depletion of intracellular potassium arrests coated pit formation and receptor-mediated endocytosis in fibroblasts. *Cell 33*, 273−285.
(24) Lindgren, C. A., Emery, D. G., and Haydon, P. G. (1997) Intracellular acidification reversibly reduces endocytosis at the neuromuscular junction. *J. Neurosci. 17*, 3074−3084.
(25) Wang, L.-H., Rothberg, K. G., and Anderson, R. G. (1993) Mis-assembly of clathrin lattices on endosomes reveals a regulatory switch for coated pit formation. *J. Cell Biol. 123*, 1107−1117.
(26) von Kleist, L., Stahlschmidt, W., Bulut, H., Gromova, K., Puchkov, D., Robertson, M. J., MacGregor, K. A., Tomilin, N., Pechstein, A., Chau, N., Chircop, M., Sakoff, J., von Kreis, J., Saenger, W., Krausslich, H. G., Shupliakov, O., Robinson, P. J., McCluskey, A., and Haucke, V. (2011) Role of the clathrin terminal domain in regulating coated pit dynamics revealed by small molecule inhibition. *Cell 146*, 471−484.
(27) Harper, C. B., Popoff, M. R., McCluskey, A., Robinson, P. J., and Meunier, F. A. (2012) Targeting membrane trafficking in infection prophylaxis: dynamin inhibitors. *Trends Cell Biol. 23*, 90−101.
(28) Hill, T. A., Odell, L. R., Quan, A., Abagyan, R., Ferguson, G., Robinson, P. J., and McCluskey, A. (2004) Long chain amines and long chain ammonium salts as novel inhibitors of dynamin GTPase activity. *Bioorg. Med. Chem. Lett. 14*, 3275−3278.
(29) Zhang, J., Lawrance, G. A., Chau, N., Robinson, P. J., and McCluskey, A. (2008) From Spanish fly to room temperature ionic liquids (RTILs): Synthesis, thermal stability and inhibition of dynamin 1 GTPase by a novel class of RTILs. *New J. Chem. 32*, 28−36.
(30) Hill, T. A., Gordon, C. P., McGeachie, A. B., Venn-Brown, B., Odell, L. R., Chau, N., Quan, A., Mariana, A., Sakoff, J. A., Chircop, M., Robinson, P. J., and McCluskey, A. (2009) Inhibition of dynamin mediated endocytosis by the dynoles - synthesis and functional activity of a family of indoles. *J. Med. Chem. 52*, 3762−3773.
(31) Gordon, C. P., Venn-Brown, B., Robertson, M. J., Young, K. A., Chau, N., Mariana, A., Whiting, A. E., Chircop, M., Robinson, P. J., and McCluskey, A. (2013) Development of second generation indole based dynamin GTPase inhibitors. *J. Med. Chem. 56*, 46−59.
(32) Hill, T. A., Mariana, A., Gordon, C. P., Odell, L. R., McGeachie, A. B., Chau, N., Daniel, J. A., Gorgani, N. N., Robinson, P. J., and McCluskey, A. (2010) Iminochromene inhibitors of dynamin I & II GTPase activity and endocytosis. *J. Med. Chem. 53*, 4094−4102.
(33) Odell, L. R., Howan, D., Gordon, C. P., Robertson, M. J., Chau, N., Mariana, A., Whiting, A. E., Abagyan, R., Daniel, J. A., Gorgani, N. N., Robinson, P. J., and McCluskey, A. (2010) The pthaladyns: GTP competitive inhibitors of dynamin I and II GTPase derived from virtual screening. *J. Med. Chem. 53*, 5267−5280.
(34) Robertson, M. J., Hadzic, G., Ambrus, J., Hyde, E., Yuri Pomè, D., Chau, N., Whiting, A. E., Robinson, P. J., and McCluskey, A. (2012) The Rhodadyn series, a new class of small molecule inhibitors of dynamin GTPase activity. *ACS Med. Chem. Lett. 3*, 352−356.
(35) Harper, C. B., Martin, S., Nguyen, T. H., Daniels, S. J., Lavidis, N. A., Popoff, M. R., Hadzic, G., Mariana, A., Chau, N., McCluskey, A., Robinson, P. J., and Meunier, F. A. (2011) Dynamin inhibition blocks botulinum neurotoxin type-A endocytosis in neurons and delays botulism. *J. Biol. Chem. 286*, 35966−35976.
(36) Macia, E., Ehrlich, M., Massol, R., Boucrot, E., Brunner, C., and Kirchhausen, T. (2006) Dynasore, a cell-permeable inhibitor of dynamin. *Dev. Cell 10*, 839−850.

(37) Quan, A., McGeachie, A. B., Keating, D. J., van Dam, E. M., Rusak, J., Chau, N., Malladi, C. S., Chen, C., McCluskey, A., Cousin, M. A., and Robinson, P. J. (2007) MiTMAB is a surface-active dynamin inhibitor that blocks endocytosis mediated by dynamin I or dynamin II. *Mol. Pharmacol. 72*, 1425−1439.
(38) Ertl, P., Jelfs, S., Muhlbacher, J., Schuffenhauer, A., and Selzer, P. (2006) Quest for the rings. In silico exploration of ring universe to identify novel bioactive heteroaromatic scaffolds. *J. Med. Chem. 49*, 4568−4573.
(39) Herman, B. D., Votruba, I., Holy, A., Sluis-Cremer, N., and Balzarini, J. (2010) The acyclic 2,4-diaminopyrimidine nucleoside phosphonate acts as a purine mimetic in HIV-1 reverse transcriptase DNA polymerization. *J. Biol. Chem. 285*, 12101−12108.
(40) Lawrence, H. R., Martin, M. P., Luo, Y., Pireddu, R., Yang, H., Gevariya, H., Ozcan, S., Zhu, J. Y., Kendig, R., Rodriguez, M., Elias, R., Cheng, J. Q., Sebti, S. M., Schonbrunn, E., and Lawrence, N. J. (2012) Development of o-chlorophenyl substituted pyrimidines as exceptionally potent aurora kinase inhibitors. *J. Med. Chem. 55*, 7392−7416.
(41) Robinson, P. J., Sontag, J.-M., Liu, J. P., Fykse, E. M., Slaughter, C., McMahon, H. T., and Südhof, T. C. (1993) Dynamin GTPase regulated by protein kinase C phosphorylation in nerve terminals. *Nature 365*, 163−166.
(42) Marks, B., and McMahon, H. T. (1998) Calcium triggers calcineurin-dependent synaptic vesicle recycling in mammalian nerve terminals. *Curr. Biol. 8*, 740−749.
(43) Quan, A., and Robinson, P. J. (2005) Rapid purification of native dynamin I and colorimetric GTPase assay. *Methods Enzymol. 404*, 556−569.
(44) Chappie, J. S., Acharya, S., Leonard, M., Schmid, S. L., and Dyda, F. (2010) G domain dimerization controls dynamin's assembly-stimulated GTPase activity. *Nature 465*, 435−440.
(45) Ogay, I. D., Lihoradova, O. A., Azimova, S., Abdukarimov, A. A., Slack, J. M., and Lynn, D. E. (2006) Transfection of insect cell lines using polyethylenimine. *Cytotechnology 51*, 89−98.
(46) van der Bliek, A. M., Redelmeier, T. E., Damke, H., Tisdale, E. J., Meyerowitz, E. M., and Schmid, S. L. (1993) Mutations in human dynamin block an intermediate stage in coated vesicle formation. *J. Cell Biol. 122*, 553−563.
(47) Dunkley, P. R., Jarvie, P. A., and Robinson, P. J. (2008) A rapid Percoll gradient procedure for preparation of synaptosomes. *Nat. Protoc. 3*, 1718−1728.
(48) Cousin, M. A., and Robinson, P. J. (2000) Ca^{2+} inhibition of dynamin arrests synaptic vesicle recycling at the active zone. *J. Neurosci. 20*, 949−957.
(49) Daniel, J. A., Malladi, C. S., Kettle, E., McCluskey, A., and Robinson, P. J. (2012) Analysis of synaptic vesicle endocytosis in synaptosomes by high content screening. *Nat. Protoc. 7*, 1439−1455.
(50) Joshi, S., Gaddipati, S., Gilbert, J., Smith, C. M., Mariana, A., Gordon, C. P., Sakoff, J. A., McCluskey, A., Robinson, P. J., Braithwaite, A. W., and Chircop, M. (2010) The dynamin inhibitors MiTMAB and OcTMAB induce cytokinesis failure and inhibit cell proliferation in human cancer cells. *Mol. Cancer Ther. 9*, 1995−2006.
(51) Stevens, D. R., Schirra, C., Becherer, U., and Rettig, J. (2011) Vesicle pools: lessons from adrenal chromaffin cells. *Front. Synaptic Neurosci. 3*, 2.
(52) Keller, P. A., Kirkwood, K., Morgan, J., Westcott, S., and McCluskey, A. (2003) The prevention of preterm labour - corticotropin releasing hormone type 1 receptors as a target for drug design and development. *Mini-Rev. Med. Chem. 3*, 295−303.
(53) Keller, P. A., Bowman, M., Dang, K. H., Garner, J., Leach, S. P., Smith, R., and McCluskey, A. (1999) Pharmacophore development for corticotropin-releasing hormone: new insights into inhibitor activity. *J. Med. Chem. 42*, 2351−2357.
(54) McCluskey, A., Keller, P. A., Morgan, J., and Garner, J. (2003) Synthesis, molecular modeling and biological activity of methyl and thiomethyl substituted pyrimidines as corticotropin releasing hormone type 1 antagonists. *Org. Biomol. Chem. 1*, 3353−3361.
(55) Hill, T. A., Odell, L. R., Edwards, J. K., Graham, M. E., McGeachie, A. B., Rusak, J., Quan, A., Abagyan, R., Scott, J. L., Robinson, P. J., and McCluskey, A. (2005) Small molecule inhibitors of dynamin I GTPase activity: Development of dimeric tyrphostins. *J. Med. Chem. 48*, 7781−7788.
(56) Robinson, P. J., Rusak, J., Quan, A., Hill, T. A., McGeachie, A. B., McCluskey, A., and Cousin, M. A. (1901) Inhibition of dynamin by bis-tyrphostin suggests two roles for GTPase activity in synaptic vesicle endocytosis. *Traffic,*.
(57) Zheng, J., Cahill, S. M., Lemmons, M. A., Fushman, D., Schlessinger, J., Cowburn, D., and Lemmon, M. A. (1996) Identification of the binding site for acidic phospholipids on the PH domains of dynamin: implications for stimulation of GTPase activity. *J. Mol. Biol. 255*, 14−21.
(58) Lin, H. C., Barylko, B., Achiriloaie, M., and Albanesi, J. P. (1997) Phosphatidylinositol (4,5)-bisphosphate-dependent activation of dynamins I and II lacking the proline/arginine-rich domains. *J. Biol. Chem. 272*, 25999−26004.
(59) Stowell, M. H., Marks, B., Wigge, P., and McMahon, H. T. (1999) Nucleotide-dependent conformational changes in dynamin: evidence for a mechanochemical molecular spring. *Nat. Cell Biol. 1*, 27−32.
(60) Scurlock, J. E., and Curtis, B. M. (1981) Tetraethylammonium derivatives: ultralong-acting local anesthetics? *Anesthesiology 54*, 265−269.
(61) Schreier, S., and Malheiros, S. V. (2000) de Paula, E. Surface active drugs: self-association and interaction with membranes and surfactants. Physicochemical and biological aspects. *Biochim. Biophys. Acta 1508*, 210−234.
(62) Chircop, M., Perera, S., Mariana, A., Lau, H., Ma, M. P. C., Gilbert, J., Jones, N. C., Gordon, C. P., Young, K. A., Morokoff, A., Sakoff, J., O'Brien, T. J., McCluskey, A., and Robinson, P. J. (2011) Inhibition of dynamin by dynole 34−2 induces cell death following cytokinesis failure in cancer cells. *Mol Cancer Ther 10*, 1553−1562.
(63) Joshi, S., Braithwaite, A. W., Robinson, P. J., and Chircop, M. (2011) Dynamin inhibitors induce caspase-mediated apoptosis following cytokinesis failure in human cancer cells and this is blocked by Bcl-2 overexpression. *Mol. Cancer 10*, 78.
(64) Schmid, S. L., and Frolov, V. A. (2011) Dynamin: Functional design of a membrane fission catalyst. *Annu. Rev. Cell Dev. Biol. 27*, 79−105.
(65) Lee, A., Frank, D. W., Marks, M. S., and Lemmon, M. A. (1999) Dominant-negative inhibition of receptor-mediated endocytosis by a dynamin-1 mutant with a defective pleckstrin homology domain. *Curr. Biol. 9*, 261−264.
(66) Ferguson, S. M., Brasnjo, G., Hyashi, M., Wolfel, M., Collesi, C., Giovedi, S., Raimondi, A., Gong, L. W., Areil, P., Paradise, S., O'Toole, E., Flavell, R., Cremona, O., Miesenbock, G., Ryan, T. A., and De Camilli, P. (2007) A selective activity-dependent requirement for dynamin 1 in synaptic vesicle endocytosis. *Science 316*, 570−574.
(67) Raimondi, A., Ferguson, S. M., Lou, X., Armbruster, M., Paradise, S., Giovedi, S., Messa, M., Kono, N., Takasaki, J., Cappello, V., O'Toole, E., Ryan, T. A., and De Camilli, P. (2011) Overlapping role of dynamin isoforms in synaptic vesicle endocytosis. *Neuron 70*, 1100−1114.
(68) Samasilp, P., Chan, S. A., and Smith, C. (2012) Activity-dependent fusion pore expansion regulated by a calcineurin-dependent dynamin-syndapin pathway in mouse adrenal chromaffin cells. *J. Neurosci. 32*, 10438−10447.
(69) Reid, A. T., Lord, T., Stranger, S. J., Roman, S. D., McCluskey, A., Robinson, P. J., Aitken, R. J., and Nixon, B. (2012) Dynamin regulates specific membrane fusion events necessary for acrosomal exocytosis in mouse spermatozoa. *J. Biol. Chem. 287*, 37659−37672.
(70) Anantharam, A., Bittner, M. A., Aikman, R. L., Stuenkel, E. L., Schmid, S. L., Axelrod, D., and Holz, R. W. (2011) A new role for the dynamin GTPase in the regulation of fusion pore expansion. *Mol. Biol. Cell 22*, 1907−1918.
(71) Chircop, M., Malladi, C. S., Lian, A., Page, S. L., Zavortink, M., Gordon, C. P., McCluskey, A., and Robinson, P. J. (2010) Calcineurin activity is required for the completion of cytokinesis. *Cell. Mol. Life Sci. 67*, 3725−3737.